Structural and electrochemical properties of Li–Ni–Co oxides synthesized by wet chemistry via a succinic-acid-assisted technique

S Castro-García[a], C Julien[b], M.A Señarís-Rodríguez[a]

a Departamento Química Fundamental, Facultade de Ciencias, Universidade de A Coruña, 15071 A Coruña, Spain

b LMDH, UMR 7603, Université Pierre et Marie Curie, 4 place Jussieu, 75252 Paris, France

International Journal of Inorganic Materials

Volume 3, Issues 4–5, July 2001, Pages 323–329

Received 17 October 2000, Accepted 20 March 2001, Available online 18 June 2001

doi:10.1016/S1466-6049(01)00040-X

Abstract

Lithiated metal oxides LiCo1−yNiyO2 were synthesized by a sol–gel method using succinic acid as chelating agent. Microcrystalline materials were formed by calcination in oxygen at 800°C. The physicochemical properties of the powders (crystallinity, lattice constants, size grain) has been investigated in the compositional range $0 \leq y \leq 1$. Structural studies show that a layered single phase was obtained. The local cationic environment has been studied by Raman and FTIR spectroscopy. The changes in the vibrational spectra are well related to those observed by X-ray diffraction. It is shown that the lithium predominant layers are preserved in the entire range of substitution. Pelletized $LiCo_{1-y}Ni_yO_2$ powders ($0.2 \leq y \leq 1.0$) were tested in Li//$LiCo_{1-y}Ni_yO_2$ cells by galvanostatic titration. These cells have an initial capacity of 140 mAh/g in the voltage range 2.8–4.2 V and show attractive charge–discharge profiles upon cycling.

Keywords

Li–Ni–Co oxides; Rechargeable Li cell; Sol–gel method

1. Introduction

The cell chemistry of Li-ion batteries based on $LiCoO_2$–graphitized carbon blend has been widely used in commercialized items, which operate in the high voltage range at ~4 V vs. Li/Li^+[1]. Problems associated with electrolyte oxidation during electrochemical processes and the relatively high price of cobalt compounds limit $LiCoO_2$ applications. A recent approach is to replace $LiCoO_2$ to improve cycling stability. The amount of work done on such research has been huge. $LiNiO_2$ is an attractive candidate: it is less oxidizing versus the electrolyte and is cheaper than the cobalt compound. However, it is very difficult to prepare it in a reproducible way because of its tendency to non-stoichiometry due to the presence of an excess of nickel. Searching for completely stable compounds and for better electrodes, the studies have been mostly directed on the base of substituted materials that are $LiCo_{1-y}Ni_yO_2$ phases, for example [2],[3], [4], [5], [6], [7], [8], [9] and [10]. These oxides alleviate the disadvantages for $LiCoO_2$ and $LiNiO_2$.

There has been a great deal of interest in preparation of $LiCo_{1-y}Ni_yO_2$ materials using wet chemistry. Currently, complexing agents are used in synthetic routes such as sol–gel, combustion, and precipitation methods [9], [10], [11] and [12]. Recently, Pereira-Ramos has critically discussed the impact afforded by low-temperature (LT) techniques especially sol–gel synthesis and precipitation techniques on the electrochemical behavior of the as prepared oxide materials [13]. Solution preparative techniques allow a better mixing of the elements and thus a better reactivity of the mixture to obtain purer products. A lower reaction temperature and shorter reaction time makes it possible to obtain compounds of high homogeneity and high specific area. Moreover, these LT methods make use of lower calcination temperatures resulting in particles of smaller size and a highly strained lattice.

The present work has focused on the synthesis of the $LiCo_{1-y}Ni_yO_2$ series of compounds by a wet-chemical procedure, namely the aqueous succinic-acid-assisted sol–gel method. Material characterization has been done by different techniques like thermal analysis, compositional analysis (ICP), X-ray diffraction (XRD) and scanning electron microscopy (SEM). Local structure and cationic environment have been

probed using Raman and FTIR spectroscopy. The electrochemical properties of $LiCo_{1-y}Ni_yO_2$ have been studied by galvanostatic measurements for the determination of charge–discharge profiles in Li//$LiCo_{1-y}Ni_yO_2$ cells.

2. Experimental

Powders of $LiCo_{1-y}Ni_yO_2$ were synthesized by a sol–gel method, via inorganic polymerization reactions in acidic solution, using succinic acid as chelating agent. Metal acetates, $M(C_2H_3O_2)_2 \cdot 4H_2O$ (M=Co, Ni), $LiC_2H_3O_2 \cdot 2H_2O$ (>99%) and succinic acid $C_4H_6O_4$ were used as starting materials.

Stoichiometric amounts of metal acetate salts were dissolved in distilled water and mixed with aqueous solutions of succinic acid using a metal:acid molar ratio of 1:1. Then, the acidic solutions were evaporated to dryness at 80°C for a few hours. The as obtained sols were decomposed by heating at 120°C to give brownish black powders, and then were heated at 400°C for a few hours to get fine grained materials of submicrometer size. The powders were slightly ground and then fired at 800°C for 2 h in air followed by a 2-h calcination in oxygen to improve the crystallinity of $LiCo_{1-y}Ni_yO_2$ final products. Powders were characterized by thermal (TG/DTA) analysis, ICP, powder XRD, SEM, Fourier transform infrared (FTIR) and Raman scattering (RS) spectroscopy.

The thermal decomposition behavior of the gels was examined by means of thermogravimetry (TG/DTA) using a STD-2960 T.A. Instruments analyser. The composition of the final products was determined using an VG PlasmaQuad II-S option induced-coupled-plasma mass-spectrometer. Powder XRD patterns were obtained with a D-5000 Siemens X-ray diffractometer, using nickel-filtered CuKα radiation (λ=1.5406 Å). The particle morphology of the materials were examined by SEM in a Jeol 6400 instrument. FTIR spectra were recorded at room temperature using an IFS113v Brucker interferometer equipped with a 3.5-μm thick beamsplitter, a globar source, and a DTGS/PE far-infrared detector; samples were ground to fine powders painted onto pellets of polyethylene slabs; data were collected in transmission mode at a spectral resolution of 2 cm^{-1} after 256 scans in vacuum atmosphere. RS spectra of the samples were collected with a U1000 Jobin-Yvon double monochromator, using the 514.5 nm laser line from the Spectra-Physics 2020 Ar-ion laser. A backscattering geometry was employed and care was taken to use a low energy laser beam to prevent reduction of

cathode materials by the laser during collection of Raman spectra. The laser power was kept below 25 mW.

Electrochemical studies were carried out on the synthesized products in order to test their suitability as cathode-active materials in high voltage lithium-containing batteries. The laboratory-scale Li//$LiCo_{1-y}Ni_yO_2$cells were fabricated employing a non-aqueous electrolyte prepared by dissolving 1 M $LiClO_4$ in propylene carbonate (PC). The typical composite cathodes consisted of the mixture of active $LiCo_{1-y}Ni_yO_2$ powders, acetylene black, and colloidal PTFE binder in the 90:5:5 weight ratio. The above mixture was pressed on to an expanded aluminum microgrid at a pressure of 500 MPa. This procedure yielded circular pellet electrodes of 10 mm diameter. The pellets were then dried at 120°C in air. Glass paper membrane was used as the separator between the cathode and the anode. Electrodes and separators were soaked in the electrolyte before being housed in a PTFE laboratory cell. Galvanostatic charge–discharge cycles were recorded using a Mac-Pile system at a slow scan mode (i.e. current pulse of 0.1 mA/cm^2 for 1 h followed by relaxation period of 0.5 h) in the potential range between 2.2 and 4.2 V.

3. Results and discussion

3.1. Thermal and compositional analysis

Fig. 1 shows two representative TG curves, for the gel precursors of the $LiCo_{0.2}Ni_{0.8}O_2$ and $LiCo_{0.6}Ni_{0.4}O_2$compounds, that were partially decomposed at 400°C before these TG measurements. In general, we observe an important weight loss at T<750°C, a plateau in the temperature range of ~750–900°C, and another weight loss at T>900°C. The first step corresponds to the decomposition of the gel and the calcination of remaining organic species, that yields well-crystallized and pure $LiCo_{1-y}Ni_yO_2$ phases. DTA data for the gels display an exothermic peak recorded around 400°C due to the decomposition of the gel formed by the metallic acetates and the succinic acid. This exothermic reaction accelerates the formation of the intermediate well-crystallized powders. Even though the crystallisation of the $LiCo_{1-y}Ni_yO_2$ phase starts below 400°C, the pure products are obtained when calcined at 800°C. Weight loss at T>900°C is due to the departure of lithium oxide from the framework. It appears that an increasing Ni content in $LiCo_{1-y}Ni_yO_2$ makes the compound thermally less stable: while for $LiCo_{0.6}Ni_{0.4}O_2$ a wide plateau exists in the

temperature range 700–1100°C, it is much narrower region for the $LiCo_{0.2}Ni_{0.8}O_2$ sample (Fig. 1).

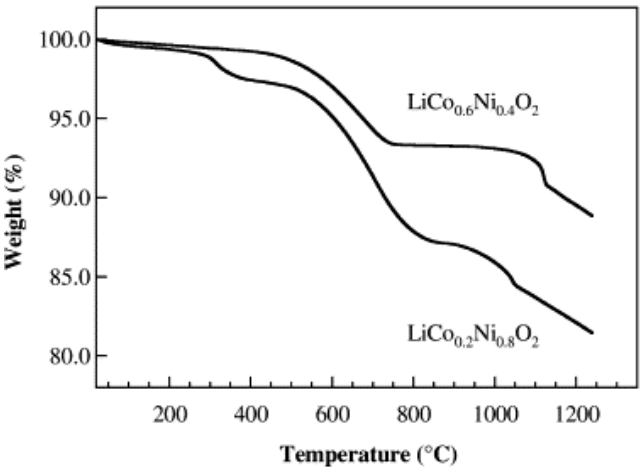

Fig. 1.
TG curves of the LiCo1−yNiyO2 (y=0.4 and 0.8) gel precursors, prepared using succinic acid as chelating agent and partially decomposed at T<400°C before TG analyses. These measurements were carried out at a heating rate of 10°C/min with oxygen flow in the range 25–1250°C.

Primary elemental analysis of the samples obtained after the thermal treatment at 800°C in oxygen are summarized in Table 1. These results show that $LiCo_{1-y}Ni_yO_2$ oxides synthesized by succinic-acid-assisted method have a composition near the ideal one for all *y* studied values.

Table 1.
Results of the elemental analysis (ICP data) of these $LiCo_{1-y}Ni_yO_2$ samples

Nominal composition	Experimental		
	Li	Co	Ni
$LiCoO_2$	0.99±0.02	1.00±0.03	–
$LiCo_{0.8}Ni_{0.2}O_2$	0.98±0.02	0.80±0.02	0.20±0.01
$LiCo_{0.6}Ni_{0.4}O_2$	1.01±0.02	0.63±0.01	0.41±0.01
$LiCo_{0.4}Ni_{0.6}O_2$	1.00±0.01	0.40±0.01	0.61±0.01
$LiCo_{0.2}Ni_{0.8}O_2$	1.00±0.01	0.20±0.01	0.83±0.02
$LiNiO_2$	1.02±0.05	–	1.03±0.05

3.2. Structure and morphology

Fig. 2 shows the XRD patterns of microcrystalline $LiCo_{1-y}Ni_yO_2$ ($0.0 \leq y \leq 0.8$) powders grown by the succinic-acid-assisted sol–gel method. Single-phase materials were obtained when the precursors were calcined up to 800°C in an oxygen atmosphere. It took at least 2 h to attain full crystallinity. Samples have a rock-salt-based structure, i.e. the layered α-$NaFeO_2$-type structure ($R\bar{3}m$ space group), with two interpenetrating close-packed fcc sublattices: one sublattice consists of oxygen anions, and the second

consists of Li and (Co, Ni) cations on alternating (111) planes. Miller indexes are given assuming an hexagonal system, in which the lithium ions are in octahedral sites between $(Co_{1-y}Ni_yO_2)_n$ infinite slabs formed by edge-sharing $(Co_{1-y}Ni_y)O_2$ octahedra. By a least-squares refinement, hexagonal lattice parameters, *a* and *c*, were calculated and plotted against nickel content (Fig. 3). For the end-member $LiCoO_2$, they are calculated to be a_{hex}=2.815 Å, c_{hex}=14.06 Å and *c*/*a*=4.995, in good agreement with values reported in the literature [14]. These cell parameters increased linearly with nickel content for $y \leq 0.8$ (this is a characteristic feature of a solid solution), while the a_{hex} increases more significantly at $y > 0.8$. $LiCo_{1-y}Ni_yO_2$ compounds ($y \leq 0.8$) obtained by this sol–gel method exhibit XRD patterns with well-defined (006)–(102) and (108)–(110) doublets. It is worth pointing that a high value of the *c*/*a* ratio ($c/a > 4.95$) and a clear splitting of the (006)–(102) and (108)–(110) Bragg lines as well as the intensity ratio $I_{(003)}/I_{(104)}$ have been acknowledged to be an indication, as far as XRD patterns are concerned, of an ordered distribution of lithium and transition-metal ions in the structure. XRD results confirm the single-phase formation of cobalt-rich cathode materials ($y \leq 0.8$), but the question of the local cationic order will be re-examined below by spectroscopic measurements.

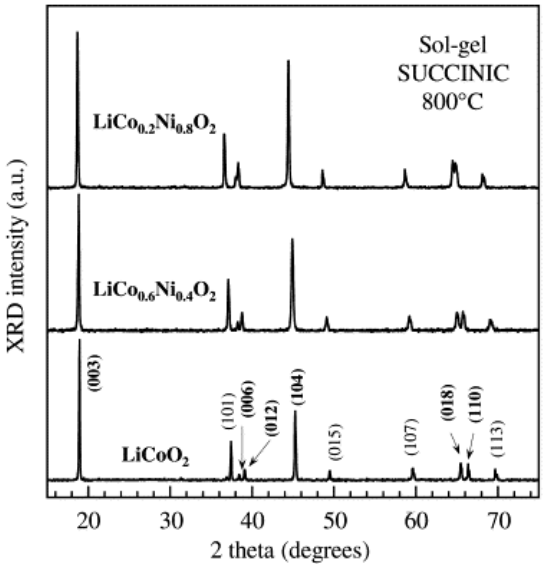

Fig. 2.
X-ray diffraction patterns as a function of cobalt substitution in the $LiCo_{1-y}Ni_yO_2$ obtained powders. XRD peaks were indexed assuming the $R\bar{3}m$ symmetry (with hexagonal indexation).

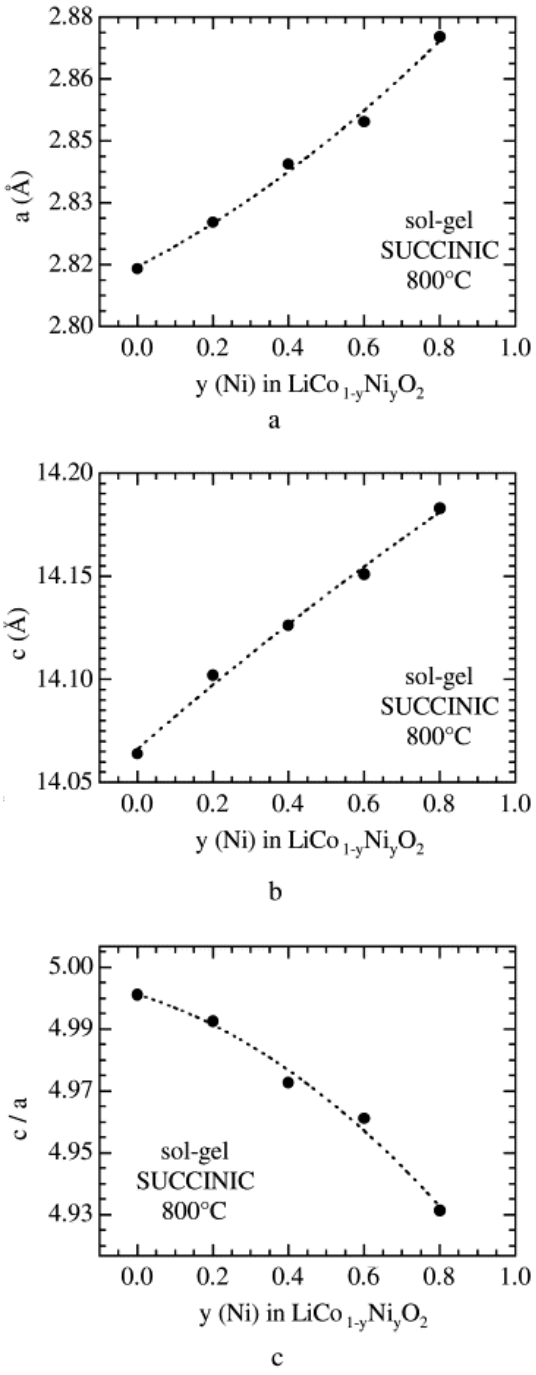

Fig. 3.
Evolution of the crystallographic parameters of the obtained LiCo1−yNiyO2 samples.

Surface morphology and texture as well as particle size were observed by scanning electron microscopy. As an example, Fig. 4 presents the typical SEM micrograph of $LiCo_{0.2}Ni_{0.8}O_2$ annealed at 800°C in oxygen. It can be seen that the individual grains are well formed and quite small, with the mean particle radius about 400 nm. These results confirm that the succinic-acid-assisted sol–gel method is well adapted for the

formation of submicron-sized particles with a narrow grain size distribution in $LiCo_{1-y}Ni_yO_2$ oxides.

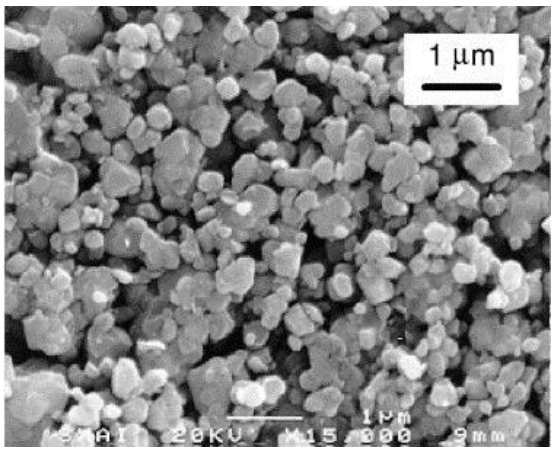

Fig. 4.
SEM picture of the obtained LiCo0.2Ni0.8O2 powders.

3.3. Vibrational spectra

The purpose of this study is to investigate the local environment of cations in a cubic close-packed oxygen array of the $LiCo_{1-y}Ni_yO_2$ lattice using FTIR and RS spectroscopy. IR and Raman modes correspond to vibrations involving primarily atomic motion of oxygen anions against their cationic neighbors [15] and [16]. Consequently, these modes are very sensitive to the cationic local environment in the host matrix.

Fig. 5 shows the RS spectrum of $LiCo_{1-y}Ni_yO_2$. For $LiCoO_2$, the RS spectrum is dominated by two strong bands located at 485 and 595 cm^{-1} which, from the group factor analysis of the D_{3d}^5 spectroscopic symmetry, are attributed to the A_{1g} and E_g species, respectively. The Raman-active modes include only the oxygen vibrations in the direction parallel (A_{1g}) or perpendicular (E_g) to the *c* axis. The high-frequency peak corresponds to the symmetric M–O stretching vibration of MO_6 groups (M=Co, Ni). As Co is substituted for Ni, the band position is shifted to lower frequency and the peak intensity vanishes due to the increase of the electronic conductivity in Ni-rich samples.

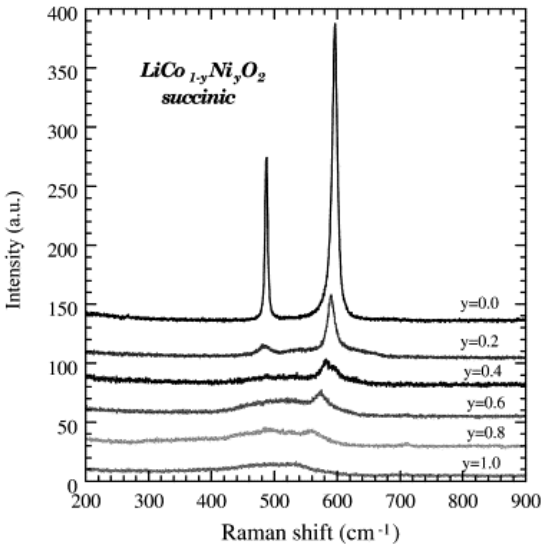

Fig. 5.

Raman scattering spectra of the obtained LiCo1−yNiyO2 samples.

Fig. 6 shows the FTIR absorption spectra of $LiCo_{1-y}Ni_yO_2$. The high-wavenumber region, at ~400–600 cm^{-1}, corresponds to the broad rock-salt band, which has broken into several distinct components. The bands located around 600 cm^{-1} are attributed to the asymmetric stretching modes of the MO_6 group, whereas bands at ~400–500 cm^{-1} are assigned to the bending modes of the O–M–O bonds. The far-infrared region, in which an isolated strong band is centered at ~240–260 cm^{-1}, is attributed to the vibration of elongated LiO_6 octahedral groups. Thus, FTIR measurements confirm XRD data showing the formation of pure $LiCo_{1-y}Ni_yO_2$ phase for $y \leq 0.8$.

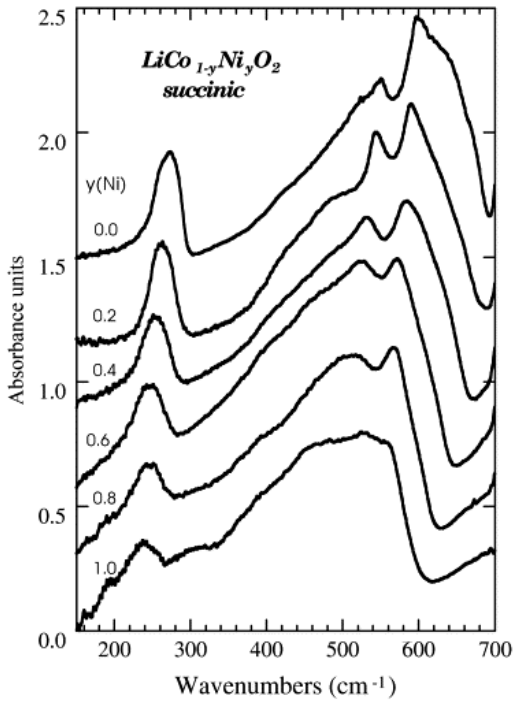

Fig. 6.

FTIR absorption spectra of the obtained LiCo1−yNiyO2 samples.

Because FTIR spectroscopy is capable of probing directly the surrounding environment of the cation, we have studied the effect of the Ni substitution on the frequency of the stretching modes in $LiCo_{1-y}Ni_yO_2$oxides (Fig. 7). The variation of the frequency modes against Ni content corresponds to features of a solid solution. In Fig. 7b, we observe a slight deviation from a linear behavior for high nickel content. This is attributed to the presence of Ni cations in the predominantly lithium layers (octahedral interstices), which disturbs the IR resonant frequency of the vibration of the O^{2-} anions against their Li^+ ion near neighbors. These results show that FTIR of $LiCo_{1-y}Ni_yO_2$ materials allows the accurate detection of short scale heterogeneity complementing the XRD results, which only provide information about the long-range structure.

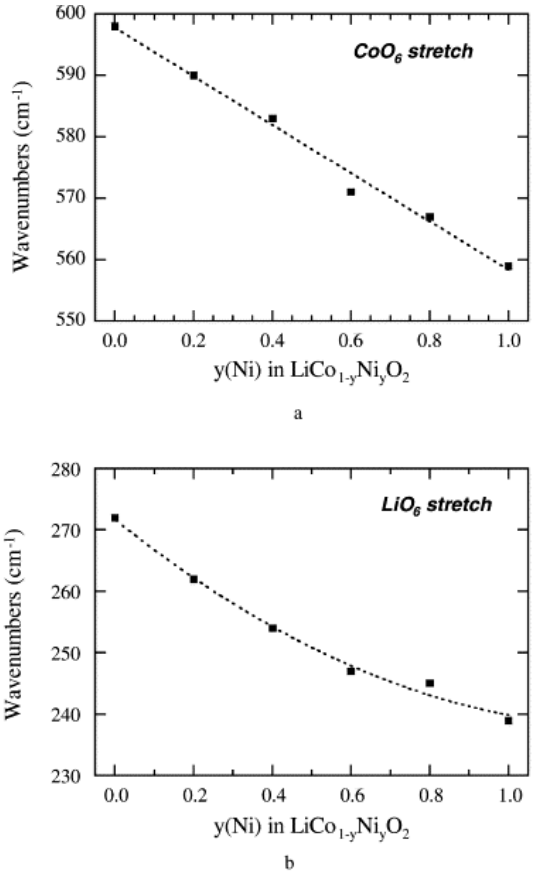

Fig. 7.
Frequency position of the infrared stretching modes of the obtained LiCo1−yNiyO2 samples as a function of the Ni substitution for Co.

3.4. Electrochemical studies

Fig. 8 shows the charge–discharge profiles of $Li//LiCo_{1-y}Ni_yO_2$ ($0.0 \leq y \leq 0.6$) cells using cathode materials prepared by this sol–gel method. The cells were charged and discharged at current densities of 0.1 mA/cm^2, while the voltage was monitored between 2.2 and 4.2 V. These experiments have been carried out at low rates to emphasize the relationship between structure and electrochemistry.

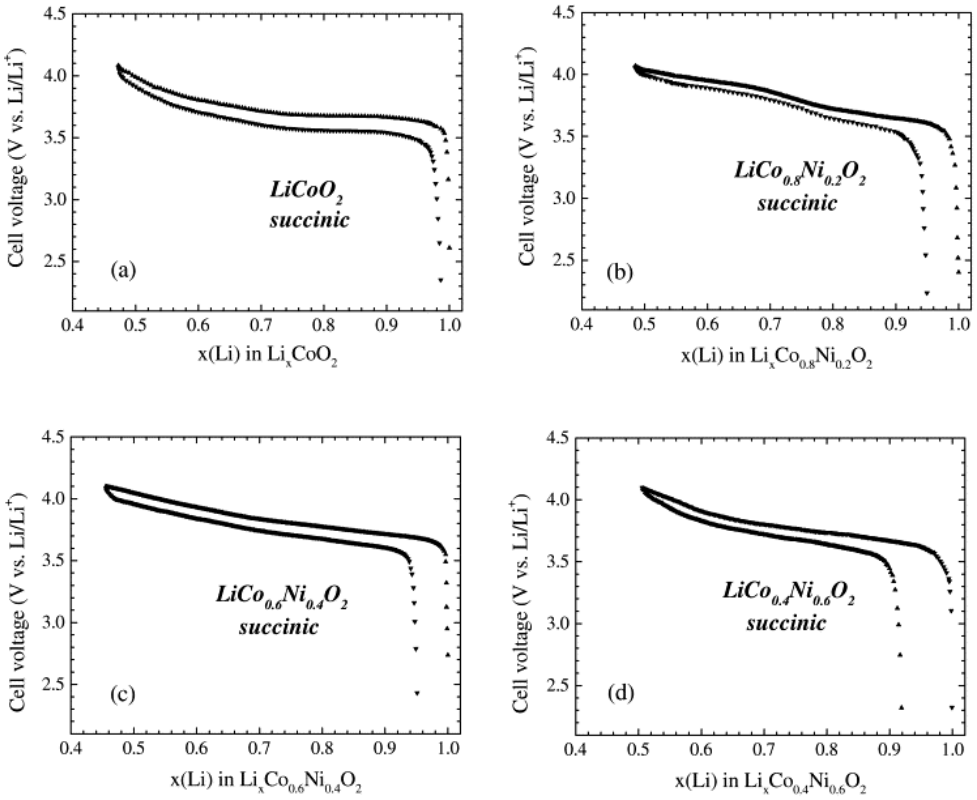

Fig. 8. Charge–discharge curves of Li//LiCo1−yNiyO2 (0.0≤y≤0.6) non-aqueous cells.

In the potential domain 2.2–4.2 V, the charge–discharge curves correspond to the voltage profiles characteristic of the LixCo$_{1-y}$NiyO$_2$ cathode materials associated with lithium occupation of the octahedral sites, in agreement with previous works [6], [7] and [8].

The similarity in the electrochemical behavior of the charge and discharge curves shows a good reversibility of the intercalation–deintercalation process during the first cycle for all studied LixCo$_{1-y}$NiyO$_2$compounds.

The fully intercalated phase is not recovered after the first discharge. The capacity retention could be probably assigned to a kinetic problem especially as the phase LixCo$_{1-y}$NiyO$_2$ is a poor electronic conductor. However, the polarization (difference in voltage between the charge and discharge curves) is very low and almost similar in all cells.

The voltage profiles of the Li//LiCo$_{1-y}$NiyO$_2$ cells are slightly different than that of Li//LiCoO$_2$. The curve obtained for LixCoO$_2$ exhibits a voltage plateau corresponding to a biphasic domain at ~3.7 V [18]. The plateau disappears for LixCo$_{1-y}$NiyO$_2$ and the monotonous variation of the potential curve reflects the existence of a LixCo$_{1-y}$NiyO$_2$ solid solution and the stabilization of the 2D framework. Reimers et

al. [17]and Saadoune et al. [18] evidenced than the occurrence of phase transitions in LixCoO$_2$ and LixNiO$_2$phases is very sensitive to the long-range Li^+ ions ordering and the substitution of Ni for Co prevents any structural change during charge–discharge in these LiCo$_{1-y}$NiyO$_2$ solid solutions.

In the case of the Li//LiCo$_{0.8}$Ni$_{0.2}$O$_2$ cell (Fig. 8b), one can distinguish the presence of two regions during the lithium insertion–extraction process. The voltage profile displays two flat domains separated by an intermediate domain characterized by a potential jump from 3.5 to 3.8 V around the composition Li$_{0.8}$Co$_{0.8}$Ni$_{0.2}$O$_2$ during the first charge. The first stage (I), near 3.5 V, is assigned to oxidation of Ni^{3+} ions, the second stage (II), near 3.8 V, is attributed to oxidation of Co^{3+} ions. In fact, in all the cobalt-rich phases, the Ni^{3+} ions are preferentially oxidized to the tetravalent state in comparison with the Co^{3+} ions, as demonstrated by Saadoune et al. [18].

The small variation of the average potential with Ni substitution for Co is shown in Fig. 9. This effect is primarily attributed to the change in the electronic structure of LiCo$_{1-y}$NiyO$_2$ compounds upon addition of Ni ions, and thus to a small variation in the Fermi level [18].

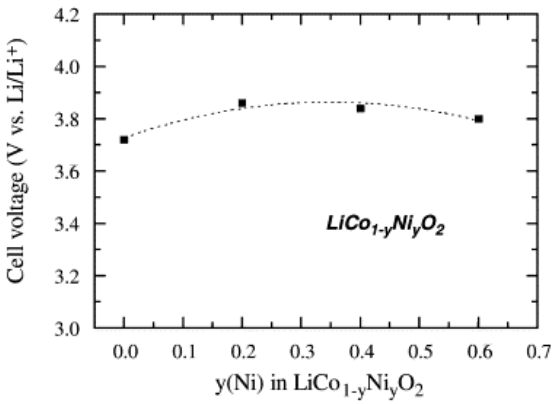

Fig. 9.
Average potential of the Li//LiCo1−yNiyO2 cells as a function of the Ni substitution for Co.

These studies also demonstrate that these cathodes yield capacities around 130–140 mAh/g close to the theoretical value of 164 mAh/g when discharged to a cut-off voltage of 2.5 V.

4. Conclusion

This work has shown that $LiCo_{1-y}Ni_yO_2$ ($0 \leq y \leq 1$) single phase materials are obtained at low temperature using the aqueous sol–gel process, in which the succinic acid acts as a chelating agent. The use of a solution process allows molecular level mixing and leads to highly uniform materials. The low-temperature technique adopted for the synthesis $LiCo_{1-y}Ni_yO_2$ cathode materials has yielded particles with small grain size around 400 nm, which favors good electrochemical performance. The charge–discharge voltage profiles of $Li//LiCo_{1-y}Ni_yO_2$ cells show good reversibility of the intercalation–deintercalation process during the first cycle and features which come from the prior oxidation of Ni^{3+} ions before the cobalt ions. These studies also demonstrated that the sol–gel synthesized-cathodes yield capacities in the range 130–140 mAh/g, close to the theoretical value 164 mAh/g, when discharged to a cut-off voltage of 2.5 V. The electrochemical properties of $LiCo_{1-y}Ni_yO_2$ cathode materials are presently being studied in the context of long term cycling.

This work shows the advantage of using wet-chemical synthetic methods for the preparation of $LiCo_{1-y}Ni_yO_2$, as materials with optimum properties can be obtained at a much-reduced cost than when using the conventional solid state method.

Acknowledgements

The authors wish to thank the Spanish and the French Foreign Office for financial support (HF1999-0101 and PAI Picasso 00717TC).

References

1. K Mizushima, P.C Jones, J.B Goodenough
   Mater. Res. Bull., 15 (1980), p. 763

2. R.J Gummow, M.M Tackeray
   Solid State Ionics, 53–56 (1992), p. 681

3. C Delmas, I Saadoune
   Solid State Ionics, 53–56 (1992), p. 370

4. T Ohzuku, A Ueda, M Nagayama, Y Iwakoshi, H Komori
   Electrochim. Acta, 38 (1993), p. 1159

5. E Zhecheva, R Stoyanova
Solid State Ionics, 66 (1993), p. 143

6. A Rougier, I Saadoune, P Gravereau, P Willmann, C Delmas
Solid State Ionics, 90 (1996), p. 63

7. C Delmas, I Saadoune, A Rougier
J. Power Sources, 43–44 (1993), p. 595

8. I Saadoune, C Delmas
J. Mater. Chem., 6 (1996), p. 193

9. B Garcia, P Barboux, F Ribot, A Kahn-Harari, L Mazerolles, N Baffier
Solid State Ionics, 80 (1995), p. 111

10. I.-H Oh, S.-A Hong, Y.-K Sun
J. Mater. Sci., 32 (1997), p. 3177

11. C Julien, M.S Michael, S Ziolkiewicz
Int. J. Inorg. Mater., 1 (1999), p. 29

12. D Mazás-Brandariz, M.A Señarís-Rodríguez, S Castro-García, M.A Camacho-López, C Julien
Ionics, 5 (1999), p. 345

13. J.P Pereira-Ramos
J. Power Sources, 54 (1995), p. 120

14. H.J Orman, P.J Wiseman
Acta Cryst., C40 (1984), p. 12

15. C Julien, A Rougier, G.A Nazri
Mater. Res. Soc. Symp. Proc., 453 (1997), p. 647

16. C Julien
Ionics, 5 (1999), p. 351

17. J.N Reimers, J.R Dahn, U Von Sacken
J. Electrochem. Soc., 140 (1993), p. 2752

18. I Saadoune, M Ménétrier, C Delmas
J. Mater. Chem., 7 (1997), p. 2505

Corresponding author. Tel.: +34-981-167-000; fax: +34-981-167-065